Title

Morphological Spectra of Adult Human Stellate Ganglia: Implications for Thoracic Sympathetic Denervation

Journal

The Anatomical Record, 301(7)

ISSN

1932-8486

Authors

Kwon, Oh Jin
Pendekanti, Shrita
Fox, Jacob N
et al.

Publication Date

2018-07-01

DOI

10.1002/ar.23797

Peer reviewed

Published in final edited form as:

Anat Rec (Hoboken). 2018 July ; 301(7): 1244–1250. doi:10.1002/ar.23797.

Morphological Spectra of Adult Human Stellate Ganglia: Implications for Thoracic Sympathetic Denervation

Oh Jin Kwon, BS[1], **Shrita Pendekanti**[1], **Jacob N. Fox, MD**[2], **Jane Yanagawa, MD**[4], **Michael C. Fishbein, MD**[5], **Kalyanam Shivkumar, MD PhD**[1], **H. Wayne Lambert, PhD**[3], **Olujimi Ajijola, MD PhD**[1]

[1]UCLA Cardiac Arrhythmia Center and Neurocardiology Research Center, Ronald Reagan UCLA Medical Center, David Geffen School of Medicine at UCLA, Los Angeles, CA, USA

[2]Department of Anesthesiology, University of Kentucky, Lexington, KY, USA

[3]Department of Neurobiology and Anatomy, West Virginia University, Morgantown, WV, USA

[4]Division of Thoracic Surgery, Department of Surgery, Ronald Reagan UCLA Medical Center, David Geffen School of Medicine, Los Angeles, CA, USA.

[5]Department of Pathology, Ronald Reagan UCLA Medical Center, David Geffen School of Medicine, Los Angeles, CA, USA.

Abstract

Background: Cardiac sympathetic denervation (CSD) to treat ventricular arrhythmias (VAs) requires transection at the middle or lower third of stellate (cervicothoracic) ganglia (SG). However, the morphological appearance of the adult SG and distribution of neuronal somata within it are not well described.

Objective: To determine the morphology of left and right SG (LSG and RSG) and the distribution of somata within.

Methods: LSG and RSG (n=28) from 14 embalmed adult cadavers were dissected intact. Weight, volume, height, morphologic appearance, relationship between C8 and T1 ganglia (which form the SG) were determined, along with histology. Demographics, history of cardiac disease, and cause of death were also reviewed.

Results: Mean age of the subjects was 76±13 years, and 5/14 were male. Three distinct morphologies of SG were identified: fusiform-rounded; fusiform-elongated; and bi-lobed. RSG and LSG did not differ in weight or volume. RSG were longer than LSG (2.05±0.28cm vs. 1.66±0.47cm, p=0.024). Bi-lobed morphology was most common in RSGs (8/14), while fused, elongated was most common in LSG (8/14). RSGs lacked fused, rounded appearance, while 28.6% of LSG appeared as such. Histologically, one focus of somata was seen in fused rounded ganglia, while fused elongated SG had somata distributed throughout. Bi-lobed SG demonstrated two foci of somata, with the interconnecting stalk containing sparse somata.

Address for Correspondence: Olujimi Ajijola, MD, PhD, UCLA Cardiac Arrhythmia Center & Neurocardiology Research Center, David Geffen School of Medicine, UCLA Medical Center, 100 Medical Plaza, Suite 660, Los Angeles, CA, 90095, Tel: (310) 206-2235, Fax: (310) 825-9092, oajijola@mednet.ucla.edu.

Conclusions: SG appear in three major forms and contain varying distributions of somata. Larger studies are warranted to define the relationship between gross anatomy and distribution of neuronal somata to improve the efficacy of CSD in treating VAs.

Keywords

cardiac sympathetic denervation; cervicothoracic ganglia; morphology; stellate ganglia; ventricular arrhythmias

INTRODUCTION

Cardiac electrophysiology is under tight control by the autonomic nervous system (ANS). The relationship between the sympathetic nervous system (SNS) and arrhythmogenesis has long been studied in animal models (Ardell et al., 2016) and in humans (Shivkumar et al., 2016). Cardiac sympathetic denervation, the removal of lower half of the stellate ganglion, and the 2nd through 4th segment (T2-T4) of the sympathetic chain (Ajijola et al., 2012a) traces its origin back almost a century (Jonnesco, 1920) for arrhythmia control; however, its efficacy still requires further investigation (Vaseghi et al., 2014).

The stellate ganglion (SG) is the fusion of the 8th cervical and first thoracic ganglia within the sympathetic chain (Janes RD, 1986; Kawashima, 2010). The first rib and subclavian artery serve as important anatomical landmarks for the SG. It is a particularly attractive nexus point for targeting sympathetic outflow to the heart (Ajijola et al., 2012b; Ajijola et al., 2012c; Vaseghi et al., 2014; Ajijola et al., 2015) given that preganglionic to postganglionic neurotransmission occurs predominantly here. In addition, its readily identifiable physical location and a wealth of previous studies supporting its role in sympathetic nervous system innervations of the heart further make the SG a clinical point of interest (Ardell et al., 2016; Shivkumar et al., 2016).

To avoid complications such as ptosis, miosis, and anhidrosis, only the lower half or distal one third of the SG along with T2-T4 are removed. However, inadequate or incorrect transection may result in persistence of the clinical problem, for example, arrhythmia recurrence (Palumbo, 1955; Ajijola et al., 2012a). As a result, understanding the anatomic variability of the SG is critical in deciding the level at which to transect.

Perlow and Vehe (Perlow and Vehe, 1935) examined the gross anatomical relationship of the sympathetic chain to surrounding structures in cadavers. They provided general descriptions of the SG (variations in length and width), and described the general relationship of the inferior cervical and first thoracic ganglia. Albert Kuntz (1927; 1929) described the thoracic ganglia as irregularly angular or fusiform, but vary greatly in form and size. Importantly, he also described nerve fibers from the first thoracic anterior (ventral) ramus traveling to the intercostal nerve (or by extension other nerves) that permit neurotransmission bypassing the SG (Kuntz, 1927; Kuntz, 1929; McCormack et al., 2011). Pather et al. (Pather et al., 2006) classified SG into three general shapes (spindle, dumbbell, and an inverted “L”), while Marcer et al. (Marcer et al., 2012) added two additional classifications (truncated and perforated); however, distributions of somata within these structures were not studied.

Despite these reports, the morphologic characteristics, based on laterality and gender and the distribution of somata within adult ganglia remain unclear.

This adult cadaveric study was undertaken to characterize SG morphology and identify the distribution of neuronal somata within the ganglion. Since the presence of cardiac pathology has been related to SG neuronal morphology (Docimo, 2008; Wood, 2010; Ajijola, 2012b; Ajijola, 2015), we also examined the hearts from the cadavers studied.

MATERIALS AND METHODS

Cadaveric Specimens

Studies involving cadavers were performed according to institutional guidelines. Bilateral SG and whole hearts were obtained from 14 formaldehyde embalmed adult cadaveric specimens from the Human Gift Registry at West Virginia University. Both the right and left stellate ganglia were identified lying anterior to the neck of the first rib on each side, and identification of the subclavian artery around which the ansae wrap. Ganglia were dissected and removed in their entirety. Demographic information, cardiovascular disease history, and cause of death were also obtained. Gross dissection of the hearts was performed by a cardiac pathologist to identify structural abnormalities.

Quantitative Measurements

Ganglia were cleaned and placed on a towel to measure morphologic properties. Ganglia were weighed, and the length of the ganglia in the superior-inferior axis was measured. Volume (in milliliter, mL) was measured by water displacement.

Histology

Bilateral stellate ganglia were paraffin embedded in a cephalo-caudad orientation, and sectioned at 5μm thickness in the coronal plane using a microtome. Five sections through the middle of the ganglion were taken, and inspected for the full length of the ganglion. Representative sections were stained with hematoxylin and eosin (H&E) to identify somata within the SG. The distribution of somata in the cephalo-caudad axis in each ganglion was recorded. Specifically, regions that contained somata were distinguished from those that only contained axon bundles. Slides were digitally scanned for analysis.

Statistical Analysis

Data are reported as mean ± standard deviation (SD) unless stated otherwise. Multi-group comparisons were evaluated using the Kruskal-Wallis ranks test for continuous variables and the Chi-square test for categorical variables. A p value < 0.05 was considered statistically significant.

RESULTS

Cadaveric characteristics

A total of 28 left and right stellate ganglia from 14 cadavers were examined. Across the cohort, mean age was 75.6 ± 13.6 years, and five were male (35.7%) (Table 1). Causes of

death included coronary artery disease or congestive heart failure in five subjects, and cardiopulmonary arrest in two others. Three subjects died from primary malignancy, and three from cerebrovascular accident or hemorrhage. The last subject had an acute fatal gastrointestinal bleed. No additional information was obtained from cardiac examinations from the subjects. Mean heart weight was 471 ± 180g, and mean left and right ventricular wall thickness were 12.5 ± 3.1mm and 4 ± 1.8mm, respectively (Table 1).

Morphological Characterization

Morphologically, the 28 stellate ganglia, independent of laterality, could be sorted into three gross categories: fusiform-rounded, fusiform-elongated, and bi-lobed (Fig. 1A). In fusiform ganglia, there is complete fusion of C8 and T1, such that the two ganglia are indistinguishable. However, as the names indicate, rounded ganglia have a spherical appearance while elongated ganglia appear finger-like (Fig. 1A). Bi-lobed SG are identified as two adjacent ganglia (superior-inferior) connected by a stalk (Fig. 1A). The distribution of these morphological categories was different between the left and right sides (Chi-square p=0.019) (Fig. 1B). Fusiform-rounded, fusiform-elongated, and bi-lobed morphologies were identified in four (28.6%), eight (57.1%), and two (14.3%) of LSG respectively. In the RSG, no fusiform-rounded morphology was identified, but fusiform-elongated and bi-lobed morphologies were identified in six (42.9%) and eight (57.1%), of RSG respectively.

Histologic analyses were performed to determine the distributions of somata within the different SG morphologies, and to support the morphological categorizations defined based on the assessment of the gross appearance of the SG. The distributions of neuron cell bodies within the SG agree with the gross morphological classifications. Fusiform-rounded and fusiform-elongated ganglia had neuronal somata distributed throughout the ganglia, while bi-lobed ganglia had two neuronal somata populations connected by a stalk (Fig. 1C). In some cases, the stalk only contained axons, while in others examples, neurons could be seen along with axons (Figs. 1C-D).

The morphological characteristics of SG (weight, volume, and length) were compared and analyzed for variations in different morphological groups (fusiform-rounded, fusiform-elongated, and bi-lobed). There was no significant difference in weight among three structures (fusiform-rounded 0.70 ± 0.25g; fusiform-elongated 0.83 ± 0.22g; bi-lobed 0.71 ± 0.22g; Kruskal-Wallis p=0.165) (Fig. 2A). Similarly, volume analyses revealed no differences (fusiform-rounded 0.64 ± 0.34mL; fusiform-elongated 0.74 ± 0.39mL; and bi-lobed 0.62 ± 0.36mL; Kruskal-Wallis p=0.405) (Fig. 2B). There were also no differences when comparing the overall length of the stellate ganglia (fusiform-rounded 1.82 ± 0.56cm; fusiform-elongated 1.89 ± 0.33cm; and bi-lobed 1.98 ± 0.46g; Kruskal-Wallis p=0.108) (Fig. 2C).

There were no differences in any of the morphological characteristics between males and females (Table 2).

Morphologic analysis by laterality

The morphologic characteristics of SG (weight, volume, length) were also compared between the right and left sides (Figs. 3A-C). There were no differences in weight (0.67 ±

0.21g vs. 0.84 ± 0.24g; Kruskal-Wallis p=0.056) and volume (0.65 ± 0.39mL vs. 0.69 ± 0.34mL; Kruskal-Wallis p=0.603) between RSG and LSG, respectively. This finding remained true when comparisons were made by morphological appearance, i.e. fusiform-elongated and bi-lobed (characteristics for fusiform-rounded SG could not compared due to its absence on the right side). However, the superior-inferior length significantly differed between sides, as RSG were significantly longer than LSG (2.05 ± 0.28cm vs. 1.66 ± 0.47cm; Kruskal-Wallis p=0.024) (Fig. 3C), likely due to the presence of more bi-lobed ganglia on the right, which are generally longer.

DISCUSSION

The major findings of the present study are that 1) SG in humans can be broadly classified into three morphologies: fusiform-rounded, fusiform-elongated, and bi-lobed; with the distribution of neuronal somata within the ganglia in agreement with this classification; and 2) the distribution of these morphologies are different between the left and right sides (no fusiform-rounded ganglia were seen on the right), with both sides frequently exhibiting different morphologies. To our knowledge, this study is the first description of these ganglia-specific characteristics. The findings of the present study may help surgeons and interventionalists minimize major adverse outcomes caused by inadequate or excessive transection or targeting of the SG during surgery or interventions. Relating the distribution of neuronal somata to the gross mnorphological appearance of the ganglion, which the surgeon or interventionalist sees, may improve efficacy for procedures involving the SG.

The SG represents the major site of pre- to post-ganglionic efferent sympathetic neurotransmission, and fibers leaving the SG can be traced to many organs such as the heart and lungs, as well as to sweat glands and vasculature in the upper extremities and thorax. Thus, several conditions, including Raynaud’s disease (Barcroft and Hamilton, 1948; Kleinsasser, 1948), (Mock and Julian, 1951; Peddie and Longmore, 1958), and cardiac arrhythmias (Ajijola et al., 2012a; Vaseghi et al., 2014), are treated by targeting the lower pole of the SG. Fibers innervating the eyelid and eyes arise from the upper pole of the SG, and resection of excessive SG can lead to complications such as ipsilateral ptosis, miosis, and enophthalmos (Peddie and Longmore, 1958). Conversely, an insufficient resection of SG can lead to recurrence of the symptoms for which the procedure was initially indicated. As such, accurate identification and description of the SG morphological spectra may aid surgeons in determining the site of transection of the SG during the stellate ganglionectomy.

The cervical sympathetic chain has long been the subject of investigation due to its therapeutic uses, and susceptibility to injury during surgical dissections in the neck (Hoffman 1957; Kiray, 2005; Civelek, 2008). Multiple studies on the cervicothoracic/stellate ganglion have identified such a ganglion in 37-100% of cadavers studied (Pather, 2006; Saylam, 2009; Zhang, 2009), however whether significant difference exist between sides is not well understood. Yin et al. compared the appearance of LSG and RSG (and cervical sympathetic chain) in Chinese cadavers, noting significant lateral asymmetry, although morphologic characteristics of the ganglia (length, width, and thickness) were similar (Yin et al., 2015). In examining the anatomic variations of the upper thoracic sympathetic chain

(including the SG), Zhang et al. found bilateral symmetry in only 16% of cases (Zhang et al., 2009).

With respect to the SG anatomy, Pather et al. observed identical SG morphologies on both sides (Pather et al., 2006), a departure from the findings of the present study. This difference may be related to the age of the cadavers in in their study (61% were < 34 weeks of age), as the morphology of the SG and differences in laterality may not be fully manifest at this early age. However, findings from Marcer et al. support the findings of the present study, showing significant morphological heterogeneity (five different shapes identified), although histologic confirmation of neuronal somata was not performed (Marcer et al., 2012). Although these studies have demonstrated anatomic dissimilarity between LSG and RSG, this study is the first to simultaneously map the adult SG morphologically and identify the distribution of neuronal somata within the ganglia histologically. The superior-inferior length of the ganglia in the present study is consistent with findings from prior studies in adults (~1.8cm) (Pather et al., 2006; Marcer et al., 2012; Yin et al., 2015). However, the RSG were slightly longer than LSG, likely related to the absence of fusiform-rounded and more bi-lobed ganglia on the right in this adult cohort.

Comparing SG in males and females, Marcer et al. reported that male ganglia were larger than ganglia in females (Marcer et al., 2012). In addition, the authors also noted that LSG were larger than RSG. These results differed from the findings in the present study, and it may be related to the larger sample size of cadavers in their study. Whether these findings may be different against histological neuronal somata distributions is not known.

A notable finding of the present study is the absence of fusiform-rounded ganglia on the right side. As a result, RSG appeared slightly longer than LSG. The absence of a particular morphology in RSG is surprising, and may be related to subtle differences in the normal anatomy of the subclavian artery, i.e. the presence of the brachiocephalic trunk on the right. The susceptibility of the morphology of SG to anatomic variations in the subclavian artery has been reported (Zhang, 2009).

Limitations

The present study focused specifically on the SG, and morphological differences between the left and right sides with respect to procedures that require transection of the SG. Whether the differences identified are driven by anatomic variations in nearby structures such as the subclavian artery requires further investigation.

Conclusions

The findings of the present study suggest that the morphology of the SG varies significantly.

Knowledge of the ganglia’s morphology may allow greater precision and accuracy in the transection of the lower half to distal third of the SG during stellate ganglionectomy to treat VAs, potentially improving both the safety and efficacy of the procedure.

ACKNOWLEGEMENTS

This work was made possible by support from NIH grants HL125730 to OAA, and HL084261 & OT2OD023848 to KS. No disclosures to report.

REFERENCES

Ajijola OA, Vaseghi M, Mahajan A, Shivkumar K. 2012a. Bilateral cardiac sympathetic denervation: why, who and when? Expert Rev Cardiovasc Ther 10:947–949. [PubMed: 23030281]

Ajijola OA, Vaseghi M, Mahajan A, Shivkumar K. 2012b. Bilateral cardiac sympathetic denervation: why, who and when? Expert review of cardiovascular therapy 10:947–949. [PubMed: 23030281]

Ajijola OA, Wisco JJ, Lambert HW, Mahajan A, Stark E, Fishbein MC, Shivkumar K. 2012c. Extracardiac neural remodeling in humans with cardiomyopathy. Circulation Arrhythmia and electrophysiology 5:1010–1116. [PubMed: 22923270]

Ajijola OA, Yagishita D, Reddy NK, Yamakawa K, Vaseghi M, Downs AM, Hoover DB, Ardell JL, Shivkumar K. 2015. Remodeling of stellate ganglion neurons after spatially targeted myocardial infarction: Neuropeptide and morphologic changes. Heart rhythm : the official journal of the Heart Rhythm Society 12:1027–1035.

Ardell JL, Andresen MC, Armour JA, Billman GE, Chen PS, Foreman RD, Herring N, O'Leary DS, Sabbah HN, Schultz HD, Sunagawa K, Zucker IH. 2016. Translational neurocardiology: preclinical models and cardioneural integrative aspects. The Journal of physiology 594:3877–3909. [PubMed: 27098459]

Barcroft H, Hamilton GT. 1948. Results of sympathectomy of the upper limb with special reference to Raynaud's disease. Lancet (London, England) 1:441–444.

Janes RD BJ, Hopkins DA, Johnstone DE, Murphy DA, Armour JA. 1986. Anatomy of human extrinsic cardiac nerves and ganglia. American journal of Cardiology 57:299–309.

Jonnesco T 1920. Angine de poitrine gukrie par la resection du sympathique cervico-thoracique. Bull Acad Med 84:1920.

Kawashima T 2010. Anatomy of the cardiac nervous system with clinical and comparative morphological implications. Anatomical Science International 86:30–49. [PubMed: 21116884]

Kleinsasser LJ. 1948. Raynaud's phenomenon and atypical causalgia; the role of sympathectomy. Annals of surgery 127:720–729.

Kuntz A 1927. Distribution of the sympathetic rami to the brachial plexus: Its relation to sympathectomy affecting the upper extremity. Archives of Surgery 15:871–877.

Kuntz A 1929. The autonomic nervous system. Philadelphia: Lea & Febiger.

Marcer N, Bergmann M, Klie A, Moor B, Djonov V. 2012. An anatomical investigation of the cervicothoracic ganglion. Clin Anat 25:444–451. [PubMed: 22488995]

McCormack AC, Jarral OA, Shipolini AR, McCormack DJ. 2011. Does the nerve of Kuntz exist? Interact Cardiovasc Thorac Surg 13:175–178. [PubMed: 21602419]

Mock CJ, Julian OC. 1951. Bilateral dorsal sympathectomy for hyperhidrosis; comparison of response to adrenalin and pilocarpine of preganglionic and post-ganglionic sympathectomy in same patient. Angiology 2:71–76. [PubMed: 14811069]

Palumbo LT. 1955. Upper dorsal sympathectomy without Horner's syndrome. AMA archives of surgery 71:743–751. [PubMed: 13268225]

Pather N, Partab P, Singh B, Satyapal KS. 2006. Cervico-thoracic ganglion: its clinical implications. Clin Anat 19:323–326. [PubMed: 16317739]

Peddie GH, Longmore DB. 1958. The treatment of hyperhidrosis by upper dorsal sympathectomy through an axillary approach. The American surgeon 24:959–963. [PubMed: 13606358]

Perlow S, Vehe KL. 1935. Variations in the gross anatomy of the stellate and lumbar sympathetic ganglia. The American Journal of Surgery 30:454–458.

Shivkumar K, Ajijola OA, Anand I, Armour JA, Chen PS, Esler M, De Ferrari GM, Fishbein MC, Goldberger JJ, Harper RM, Joyner MJ, Khalsa SS, Kumar R, Lane R, Mahajan A, Po S, Schwartz PJ, Somers VK, Valderrabano M, Vaseghi M, Zipes DP. 2016. Clinical neurocardiology defining

the value of neuroscience-based cardiovascular therapeutics. The Journal of physiology 594:3911–3954. [PubMed: 27114333]

Vaseghi M, Gima J, Kanaan C, Ajijola OA, Marmureanu A, Mahajan A, Shivkumar K. 2014. Cardiac sympathetic denervation in patients with refractory ventricular arrhythmias or electrical storm: intermediate and long-term follow-up. Heart rhythm : the official journal of the Heart Rhythm Society 11:360–366.

Yin Z, Yin J, Cai J, Sui T, Cao X. 2015. Neuroanatomy and clinical analysis of the cervical sympathetic trunk and longus colli. J Biomed Res 29:501–507. [PubMed: 26668584]

Zhang B, Li Z, Yang X, Li G, Wang Y, Cheng J, Tang X, Wang F. 2009. Anatomical variations of the upper thoracic sympathetic chain. Clin Anat 22:595–600. [PubMed: 19418453]

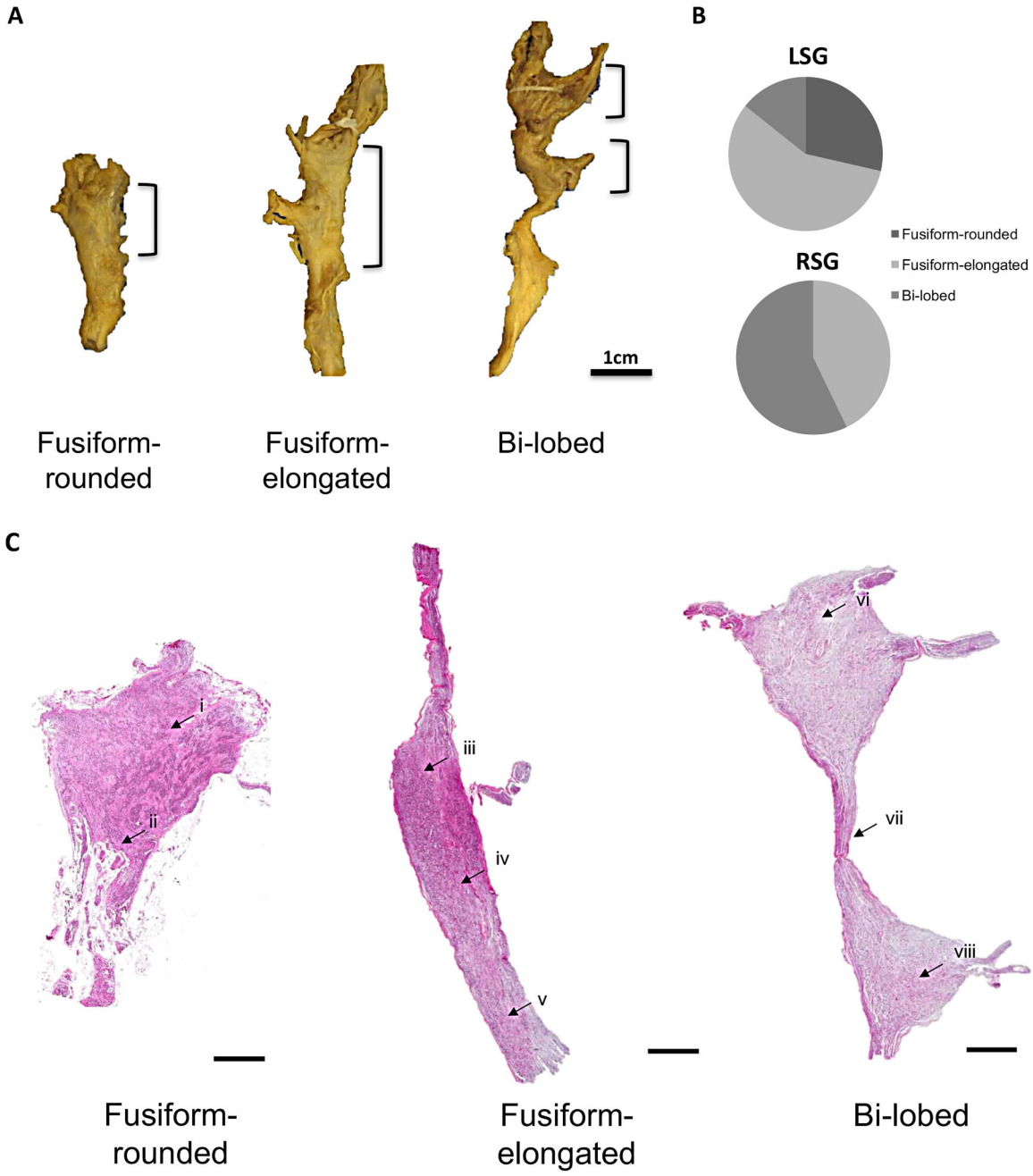

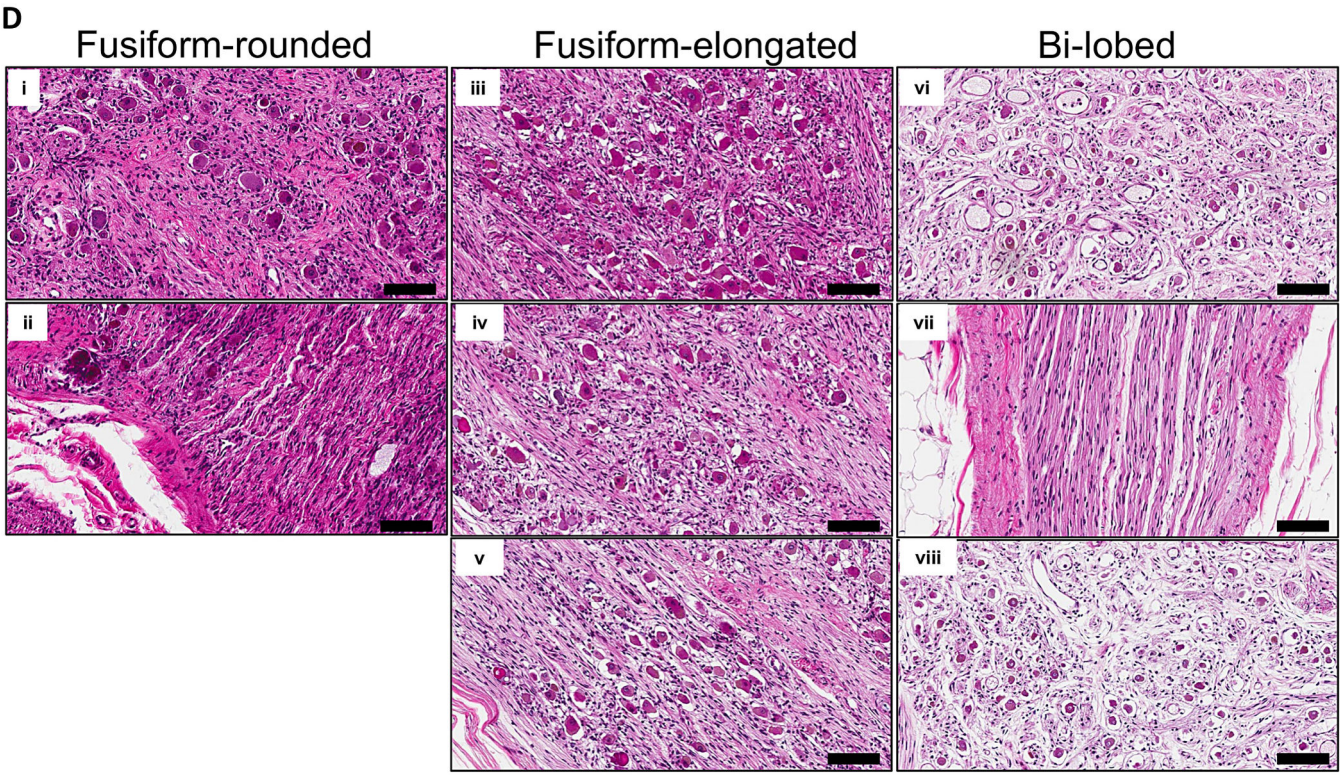

Figure 1. Morphological Characterization of Human Stellate Ganglia.

A. Representative images of the three major morphological groups of stellate (cervicothoracic)ganglia identified are shown. Scale bar: 1cm. **B.** Distribution of morphologies in left and right SG (LSG and RSG, respectively). **C.** Representative histologic sections showing the distribution of neurons within the morphologies of ganglia observed. **D.** Magnified image of neurons and axons from the regions shown in panel C. Scale bar: 100μm.

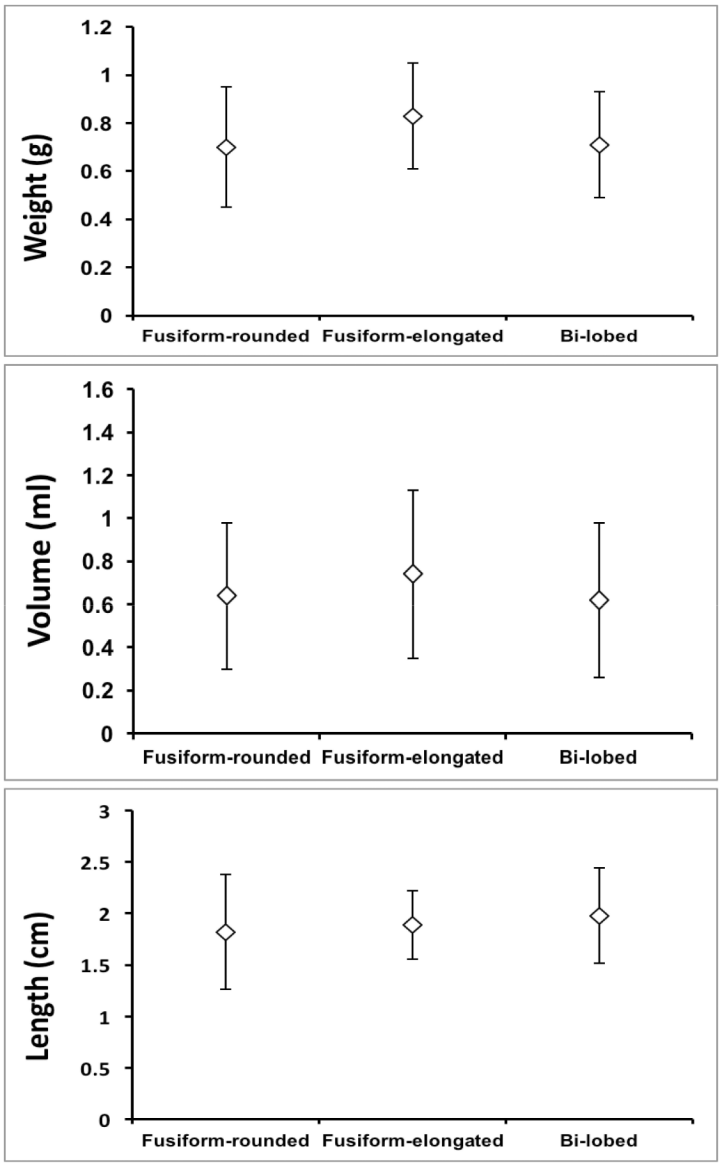

Figure 2. Morphologic Characteristics of Ganglia by Morphological Class.

A-C. Mean weight, volume, and length (rostra-caudal axis) of stellate (cervicothoracic) ganglia from cadaveric dissection, respectively. Data shown are mean ± standard error.

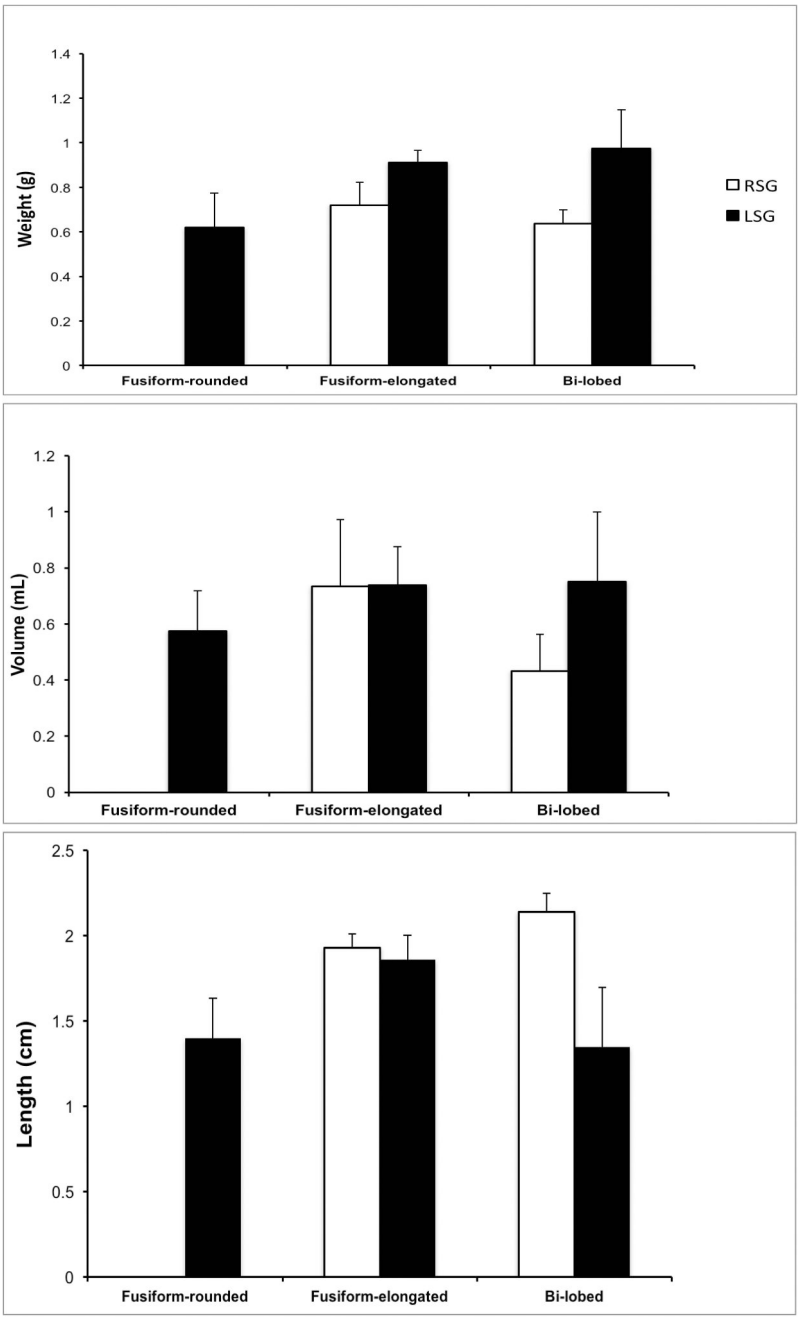

Figure 3. Characteristics of Right and Left Stellate Ganglia.

The differences in morphological characteristics of right and left stellate (cervicothoracic) ganglia are shown in **A-C**, representing weight, volume, and length (rostra-caudal axis), respectively. Data shown are mean ± standard deviation. *p=0.024.

Table 1.

Patient Characteristics

Variables	Patient (N=14)
Age (years)	75.6 ± 13.6
Male Sex	5 (35.7%)
Heart Weight (g)	471.1 ± 179.7
Left Ventricle Thickness (mm)	12.5 ± 3.1
Right Ventricle Thickness (mm)	4 ± 1.8

Data presented as mean ± standard deviation or number (percentage).

Comparisons for continuous variables were made using the Kruskal-Wallis rank test and comparisons for categorical variables were made using the Pearson chi-square test.

* Indicates statistical significance at $p<0.05$.

Table 2.

Stellate Ganglia Characteristics by Gender

	Male (N=5)	Female (N=9)	p-value
Stellate Weight (g)	0.83 ± 0.18	0.71 ± 0.25	0.179
Stellate Volume (mL)	0.79 ± 0.43	0.61 ± 0.31	0.138
Height (cm)	1.93 ± 0.42	1.81 ± 0.44	0.358
RSG			
Fusifom-rounded	0 (0%)	0 (0%)	-
Fusiform-elongated	3 (60%)	3 (33.3%)	-
Bi-lobed	2 (40%)	6 (66.7%)	-
Weight (g)	0.78 ± 0.18	0.61 ± 0.20	-
Volume (mL)	0.78 ± 0.47	0.58 ± 0.35	-
Height (cm)	2.1 ± 0.24	2.02 ± 0.31	-
LSG			
Fusiform-rounded	2 (40%)	2 (22.2%)	-
Fusiform-elongated	2 (40%)	7 (77.7%)	-
Bi-lobed	1 (20%)	1 (11.1%)	-
Weight (g)	0.89 ± 0.20	0.81 ± 0.27	-
Volume (mL)	0.8 ± 0.45	0.63 ± 0.28	-
Height (cm)	1.76 ± 0.51	1.6 ± 0.47	-

Data presented as mean ± standard deviation or number (percentage).

Comparisons for continuous variables were made using the Kruskal-Wallis rank test and comparisons for categorical variables were made using the Pearson chi-square test.

* Indicates statistical significance at $p<0.05$.